Earth Syst. Dynam. Discuss., 6, 2617–2643, 2015
www.earth-syst-dynam-discuss.net/6/2617/2015/
doi:10.5194/esdd-6-2617-2015

Earth System Dynamics Discussions
Open Access

Atmospheric rivers moisture transport from a Lagrangian perspective

A. M. Ramos[1], R. Nieto[2], R. Tomé[1], L. Gimeno[2], R. M. Trigo[1], M. L. R. Liberato[1,3], and D. A. Lavers[4]

[1]Instituto Dom Luiz, Faculdade de Ciências, Universidade de Lisboa, Lisbon, Portugal
[2]EPhysLab (Environmental Physics Laboratory), Facultade de Ciencias, Universidade de Vigo, Ourense, Spain
[3]School of Sciences and Technology, University of Trás-os-Montes e Alto Douro, Vila Real, Portugal
[4]Center for Western Weather and Water Extremes, Scripps Institution of Oceanography, University of California, San Diego, La Jolla, California, USA

Received: 2 December 2015 – Accepted: 8 December 2015 – Published: 17 December 2015

Correspondence to: A. M. Ramos (amramos@fc.ul.pt)

Published by Copernicus Publications on behalf of the European Geosciences Union.

Atmospheric rivers moisture transport from a Lagrangian perspective

A. M. Ramos et al.

Abstract

An automated atmospheric rivers (ARs) detection algorithm is used for the North Atlantic Ocean Basin allowing the identification of the major ARs that affected western European coasts between 1979 and 2014 over the winter half-year (October to March). The entire west coast of Europe was divided into five domains, namely, the Iberian Peninsula (9.75° W; 36–43.75° N), France (4.5° W; 43.75–50° N), UK (4.5° W; 50–59° N), southern Scandinavia and the Netherlands (5.25° E; 50–59° N), and northern Scandinavia (5.25° E; 59–70° N). Following the identification of the main ARs that made landfall in western Europe, a Lagrangian analysis was then applied in order to identify the main sources of moisture that reach each domain. The Lagrangian dataset used was obtained from the FLEXPART model global simulation from 1979 to 2012, where the atmosphere was divided into approximately 2.0 million parcels, and it was forced by ERA-Interim reanalysis on a 1° latitude–longitude grid.

Results show that, in general, for all regions considered, the major climatological source of moisture extends along the subtropical North Atlantic, from the Florida Peninsula (northward of 20° N), to each sink region, with the nearest coast to each sink region always appearing as a local maximum of evaporation. In addition, during the AR events, the Atlantic subtropical source is reinforced and displaced, with a slight northward movement of the moisture sources is found when the sink region is positioned at higher latitudes. In conclusion, the results confirm the advection of moisture linked to ARs from subtropical ocean areas, but also the existence of a tropical one, and the mid-latitude sources further the analysed longitude along the North Atlantic is located eastward.

ESDD
6, 2617–2643, 2015

1 Introduction

Atmospheric rivers (ARs) are relatively narrow (~ 500 km) pathways of water vapour (WV) transport that can extend for thousands of kilometres and contain large amounts of WV and are often accompanied by strong winds (Zhu and Newell, 1998; Ralph et al., 2004). According to Ralph et al. (2004, 2005), AR properties include a concentred band of enhanced WV in the lower troposphere and a pre-cold frontal low level jet (LLJ) due to the temperature gradient across the cold front.

The attribution of the terms atmospheric or tropospheric rivers rose some debate by Wernli (1997) and Bao et al. (2006). Recently, an agreement has moved (Dettinger et al., 2015) regarding the relationships among ARs, warm conveyor belts (WCBs), and tropical moisture exports (TMEs). TMEs are zones of intense vapour transport out of the tropics, vapour that is frequently conducted by ARs toward cyclones and WCBs. TMEs can provide important vapour sources for ARs, but most ARs also incorporate mid-latitude sources and convergences of vapour along their paths (Dettinger et al., 2015).

The detection of ARs can be achieved adopting two considerably different approaches, namely: (a) using integrated column water vapor (IWV) (e.g. Ralph et al., 2004; Ralph and Dettinger, 2011), and (b) based on the use of the vertically integrated horizontal water vapor transport (IVT) (e.g. Zhu and Newell, 1998; Lavers et al., 2012; Ramos et al., 2015).

The importance of ARs in extreme precipitation events and floods has been analysed in detail for the US west coast (particularly for the California) over the last decade (e.g. Dettinger et al., 2011; Neiman et al., 2008; Ralph et al., 2013). In western Europe, ARs have been recently studied from a climatological point of view for the UK (Lavers et al., 2011, 2012) and for the Iberian Peninsula where Ramos et al. (2015) studied its relationship with extreme precipitation. In addition, the importance of ARs in a few particular cases of extreme precipitation in Europe has also been analysed (Liberato

ESDD
6, 2617–2643, 2015

et al., 2012; Stohl et al., 2008) including some important historical cases (e.g. Trigo et al., 2014).

The increasing attention to the AR topic is confirmed by the publication of two recent reviews, with Ralph and Dettinger (2011) putting emphasis on the multiple analyses produced for the ARs striking the western coast of USA, while Gimeno et al. (2014) have focused on the structure, methods for detection, impacts, and dynamics of ARs.

Bao et al. (2006) proposes that moisture present in the ARs has two main origins: local moisture convergence along the front of extra-tropical cyclones, and direct pole-ward transport of tropical moisture suggesting that the ARs play an important role in the water cycle especially in transporting moisture from the tropics to mid and high latitudes. In this context Dacre et al. (2015), has analysed selected cases of the transport of water vapour within a climatology of wintertime North Atlantic extra-tropical cyclone. It is discussed the possibility that ARs are formed by the cold front that sweeps up water vapour in the warm sector as it catches up with the warm front. This causes a narrow band of high water vapour content to form ahead of the cold front at the base of the warm conveyor belt airflow. Thus, according to Dacre and colleagues, water vapour in the cyclone's warm sector, not long-distance transport of water vapour from the subtropics, is responsible for the generation of ARs.

To the best of our knowledge works dealing with moisture transport and sources along the ARs are scares and were only done mainly for selected case studies. For instance, Moore et al. (2012) used Lagrangian trajectories associated with heavy flooding rainfall in Nashville to analyse if they were connected with ARs events. Stohl et al. (2008) studied the remote sources of water vapour forming precipitation on the Norwegian and their link with ARs on a 5 year period. Sodemann and Stohl (2013) analysed the moisture origin and meridional transport in ARs and their association with multiple cyclones for December 2006. Knippertz and Wernli (2010), present a Lagrangian climatology of tropical moisture exports to the Northern Hemispheric extra-tropics by analysing forward trajectories leaving a box between 0 and 20° N spanning from 1979–2001. These researches base their result on the use of Lagrangian models

ESDD
6, 2617–2643, 2015

which are able to model the evolution of the moisture in the atmosphere along several trajectories. The use of Lagrangian models such as, FLEXPART (Stohl et al., 1998), can help to assess the main sources of moisture and its transport within the ARs. This Lagrangian model allows following the moisture that reaches a specific region, more specifically is it possible to know changes in the specific humidity along the trajectories in time. Knowing the specific moisture (q) in every time step it is possible identify the particles that loose moisture through precipitation (p), or receive it through evaporation (e). FLEXPART can "transport" the particles backward or forward in time using a 3-D wind field. The account of evaporation minus precipitation permits knowing the sources of moisture (when evaporation is higher than precipitation) and sinks (contrary case).

The Lagrangian methodology of moisture source based on FLEXPART has been extensively used in the last decade for both regional studies (e.g. Nieto et al., 2006) and global ones (Gimeno et al., 2010). The comprehensive review by Gimeno et al. (2012) provides details of the uncertainty and significance of this Lagrangian approach, as well as a comparison with other methods of estimating moisture sources and the original paper by Stohl et al. (2004) provides further information on FLEXPART model.

Here we are mainly interested in analysing the backward trajectories that arrive in the various regions along the Atlantic coast of Europe where ARs make their landfall. The objectives of this work are twofold: (1) to identify the ARs affecting the western European coast between 1979–2012 during the winter half-year (ONDJFM) and, (2) to provide a comprehensive analysis of AR moisture sources and transport in the winter half-year over the different European domains.

The work is organized as follows: in Sect. 2 the datasets and the different methodologies are presented while Sect. 3 analyses the ARs that landfall in Europe. The ARs moisture transport for the ARs that reach Europe is analysed in Sect. 4. Finally the conclusions are presented in Sect. 5.

ESDD
6, 2617–2643, 2015

2 Methods and datasets

2.1 Atmospheric river detection

We have used the ERA-Interim reanalysis (Dee et al., 2011) with a 0.75° latitude–longitude grid resolution, spanning from 1979–2012 for the winter half-year (October to March (ONDJFM) for the detection of the ARs. The variables used at a 6 h time steps were: the humidity (q), zonal (u) and meridional (v) winds at 1000, 925, 850, 700, 600, 500, 400 and 300 hPa levels since most of the moisture are accounted in these levels.

The ARs detection scheme employed (Lavers et al., 2012; Ramos et al., 2015) depends entirely on the vertically integrated horizontal water vapour transport (IVT) and was computed between the 1000 and the 300 hPa levels (Eq. 1):

$$\mathrm{IVT} = \sqrt{\left(\frac{1}{g}\int_{1000\,\mathrm{hPa}}^{300\,\mathrm{hPa}} q u\,\mathrm{d}p\right)^2 + \left(\frac{1}{g}\int_{1000\,\mathrm{hPa}}^{300\,\mathrm{hPa}} q v\,\mathrm{d}p\right)^2}, \tag{1}$$

where q is the specific humidity, u and v the zonal and meridional layer averaged wind while dp is the pressure difference between two adjacent levels. Finally, g is the acceleration due to gravity.

The identification of the ARs was performed as in Lavers and Villarini (2013) and Ramos et al. (2015), but considering three distinct meridian reference domains (Fig. 1a) centred respectively at: 9.75° W (just west of both Iberian Peninsula and Ireland), 4.50° W (located west of UK and France) and 5.25° E (west of Scandinavia). Each different meridian domain (Fig. 1a) was further divided into 10° sections between 35 and 75° N for the 9.75 and 4.50° W, and between 50 and 70° N for the Scandinavia domain (5.25° E) to allow for different latitude dependent IVT.

The latitude IVT threshold, for the 9.75° W meridian domain, was computed by taking the daily maximum IVT between 35 and 75° N (over the 9.75° W) at 12:00 UTC on each day between 1979–2012 and binned it into 10° latitude sectors. Following Lavers et al. (2012) the 85th percentile of the IVT in each latitude sector was used as the

ESDD
6, 2617–2643, 2015

threshold value of the AR identification, since this percentile was associated with the most intense ARs. For the other meridian domains a similar procedure was adopted with the derived thresholds for the different domains and sectors summarized in Table 1.

With the distinct thresholds computed for the different domains the following detection scheme was applied for each sector:

- At each 6 h time step between 1979 and 2012 over the winter half-year, we compared the IVT values at grid points for each different domain and extracted the maximum IVT value and location.

- If the maximum IVT exceeded the local IVT threshold (Table 1), this particular grid point was highlighted. We then performed a backward/forward search to identify the maximum IVT at each longitude and tracked the location for the grid points where the local IVT threshold was exceeded. However, ARs must extend over 1500 km, therefore a minimum length threshold was also imposed. This condition is checked every 6 h and we considered it an AR time step when it is fulfilled. In this case, it corresponds to 30 contiguous longitude points ($30 \cdot 0.75^\circ = 20.25^\circ \sim$ 1600 km, considering that at 55° N the length of a degree of longitude is $\sim$ 71 km);

- With all the AR time steps identified for the different domains, only the persistent AR events will be retained. For a persistent AR event to occur (Lavers and Villarini, 2013; Ramos et al., 2015) a minimum temporal criteria must be fulfilled: (1) it must have at least 18 h persistence (three continuous time steps) and (2) to be independent, that is two persistent ARs were considered distinct only if they were separated by more than 1 day (four time steps).

The number of persistent ARs identified for each domain is summarized in Table 1 (last column) and will be discussed in Sect. 3.

ESDD
6, 2617–2643, 2015

2.2 Lagrangian moisture transport

The method developed by Stohl and James (2004) was used in this work which allows tracking the atmospheric moisture along Lagrangian trajectories of air parcels in the atmosphere. The Lagrangian dataset used, come from a Lagrangian model FLEXPART v9.0 global simulation from 1979 to 2012, in which the atmosphere was divided into approximately 2.0 million parcels, and it was forced by the 1° latitude–longitude grid ERA-Interim reanalysis (Dee et al., 2011) available every 3 h. The output of the FLEXPART simulation, consist in four daily outputs (at times 00:00, 06:00, 12:00 and 18:00 UTC).

The Lagrangian mentioned method divides the atmosphere homogeneously into a large amount of air parcels (particles), where each one represents a fraction of the total atmospheric mass. These particles are then advected using the reanalysis wind field while the other meteorological properties of the air parcel (e.g. specific humidity and temperature) are also processed by FLEXPART model.

The changes on the specific moisture (dq) of a particle (with mass m) along the time (dt) during its trajectory can be expressed as (Eq. 2):

$$e - p = m\frac{\mathrm{d}q}{\mathrm{d}t}, \quad (2)$$

where $(e - p)$ can be inferred as the freshwater flux in the parcel (the difference of evaporation and precipitation). Each particle is tracked backwards for a transport time of 10 days because that is the average residence time of water vapour in the atmosphere (Numaguti, 1999).

The moisture changes $(e - p)$ of all of the particles in the atmospheric column over a specified area (A) gives the surface freshwater flux ($E - P$), where E is the evaporation rate per unit area, P is the precipitation rate per unit area (Eq. 3):

$$E - P \approx \frac{\sum_{k=1}^{K}(e - p)}{A}, \quad (3)$$

ESDD
6, 2617–2643, 2015

where K is the total number of particles in the atmospheric column (∼ 2 million in our experiment).

The different areas where the ARs make landfall will be discussed in Sect. 3, while the selection of each domains where the particles will be selected for the backwards trajectories ($E-P$) analyses is going to be discussed in Sect. 4.

3 Landfall of atmospheric rivers in Europe

Following the application of the various steps of the method explained in the previous Sect. 2, for all the different domains, the IVT threshold and the number of ARs considered for each domain is summarized in Table 1. There were 271 ARs over the Iberian Peninsula/Ireland domains, with a maximum of 87 ARs on the 45–55° N sector; for the UK/France domain the total number is 351, with the maximum of 98 ARs observed at the latitudes between 55 and 65° N. In the case of Scandinavia, and since the ARs come from the Atlantic region, we chose to divide the domain in two sectors (50 to 60° N and 60 to 70° N), with the maximum number of ARs being recorded at the 50–60° N sectors (100 ARs).

This first assessment of ARs for the different domains confirms the results in Lavers and Villarini (2013), namely that the ARs also strike other regions of Europe and not only the Iberian Peninsula (Ramos et al., 2015) or the UK (Lavers et al., 2011). In any case, we are confident that the use of three different meridians of control (9.75, 4.5° W and 5.25° E provides a finer and more robust assessment of all the ARs that make landfall in Europe. This will be very helpful in Sect. 4 where the study of the ARs moisture transport will be analysed in detail, since the specific location where the ARs made landfall is of most importance. Taking this into account, and since the we were particularly interested in the ARs that have impacts over land we havereorgazined the ARs previously computed (Fig. 1a and Table 1) into the following new 5 domains (Fig. 1b), identified: (1) *Iberian Peninsula* (9.75° W; 36–43.75° N); (2) *France* (4.5° W; 43.75—50° N); (3) *UK* (4.5° W; 50–59° N); (4) *southern Scandinavia and the*

ESDD
6, 2617–2643, 2015

Netherlands (5.25° E; 50–59° N) and (5) *northern Scandinavia* (5.25° E; 59–70° N). This allows having contiguous domains from 36 to 70° N, with domains (3) and (4) only changing the meridional reference maintaining the latitudinal division. An analysis in Table 2, shows the number of ARs and the correspondent ARs times steps for each new domain that will be analysed in detailed in Sect. 4. This varies from 21 ARs (117 time steps) in the Iberian Peninsula domain and the 140 ARs (665 time steps) in the France domain.

The IVT threshold has a maximum around the 45 and 55° N for all meridian domains which is in good agreement with the results obtain by Lavers and Villarini (2013) near to 10° W. In addition, this maximum is also confirmed by the analysis of the seasonal IVT mean fields, where a maximum between 45 and 55° N is present (not shown).

In order to have the perception of the path of the ARs, we have computed the maximum longitudinal IVT for each ARs, in order to have a first guess of the position of the ARs along the North Atlantic Ocean. For every new domain, we have computed the median, 90th percentile and 10th percentile of the maximum IVT positions of the different ARs along their first guess trajectories and the results are presented in Fig. 2. The use of the 90th and 10th percentile allows one to visualize the spread in positions of the vast majority of the ARs along the North Atlantic basin associated to each domain.

Regarding the Iberian Peninsula (Fig. 2a), the median position of the ARs is mainly zonal, with a small NW component, while the spatial dispersion is quite high, especially as we move from the landfall area. This NW component is in line with the results obtain by Ramos et al. (2015), where a positive anomaly of Sea Level Pressure is found south of Portugal when the ARs make landfall in the Iberian Peninsula.

In the cases of France and UK (Fig. 2b), the paths and dispersions are similar with respect to the median path of the ARs especially on the East North Atlantic domain. The main differences are closer to the two domains, namely: (1) a more zonal path associated to the France domain, while for the UK its path near the reference meridian is clearly more SW-NE oriented, and (2) the dispersion of the ARs path are higher in the UK domain then in the France one, particularly west of 40° W. The results for

ESDD
6, 2617–2643, 2015

the UK confirm those obtained by Lavers et al. (2011) but here we have used the full climatology while Lavers et al. (2011) only analysed the ARs path of selected cases. Concerning the last two domains (Fig. 2c), results are very similar with the ones obtained for France and UK domains, i.e. most ARs show a strong SW-NE orientation, east of 40° W particularly for the ARs that arrive in the north Scandinavian domain. In addition, the dispersion of the paths in these two domains is relatively higher than for the other three domains.

These five new domains (Fig. 1a) are the ones that will be used in the computation of the ARs moisture transport that make landfall over the western coasts of the analysed Europe domains.

4 Atmospheric rivers moisture transport

The use of the FLEXPART simulations and the computation of the $E-P$, intends to find the origin of the moisture associated with the ARs reaching the Atlantic European coast. As we are interested in the effective moisture sources the analysis is restricted to areas where evaporation exceeds precipitation, i.e. $(E-P) > 0$ clearly depicted in colour in Figs. 3 and 4.

The $E-P$ backward trajectories analysis were performed for air particles residing over the western 5° from the ARs detection meridian reference (Table 3): e.g. for the Iberian Peninsula region it includes particles located inside a rectangle (spreading between 9.75 and 4.75° W and from 36 to 43.75° N) on a 6 hourly basis.

For each domain, two very different $E-P$ computations were performed: (a) the $E-P$ climatological $(E-P)_{\mathrm{Cli}}$ computation for each Julian day where an AR occurs, and b) the $E-P$ composite $(E-P)_{\mathrm{AR}}$ for all the AR days. In addition, the $E-P$ anomaly $(E-P)_{\mathrm{An}}$ was also computed by simply obtaining the difference between $(E-P_{\mathrm{AR}})-(E-P_{\mathrm{Cli}})$. A comprehensive representation of the fields of $(E-P)_{\mathrm{Cli}}$ and $(E-P)_{\mathrm{An}}$, for all the five studied regions is provided in Fig. 3 (left panels) and Fig. 3 (right panels), respectively. In general, for all the regions, the major climatological source of moisture extends

ESDD
6, 2617–2643, 2015
Atmospheric rivers moisture transport from a Lagrangian perspective
A. M. Ramos et al.

along the subtropical north Atlantic (from the Tropic of Cancer to 35° N according to the American Meteorological Society' definition), from the Gulf Stream Current, just off the Florida Peninsula (northward 20° N), to each sink region, being farther southward (clearly subtropical) on the west basin of the North Atlantic Ocean and reaching extra-tropical latitudes on the east basin coast. Moreover, the nearest coast to each sink region is always appearing as a local maximum of evaporation; (e.g. see the southern Iberian Peninsula coast or the Biscay Gulf for France). The Norwegian Sea acts as a more important source as the region analysed is located at higher latitudes, reaching a maximum for the north Scandinavia region. The importance of the North Atlantic Ocean as a source of moisture for some regions of Europe has already been noticed in previous works. In a complete moisture source catalogue for important climate regions Castillo et al. (2014) showed that for southern Europe (including our Iberian Peninsula and France regions) and the northern Europe (UK, southern Scandinavia and the Netherlands, and northern Scandinavia) the dominant source of moisture is the northern Atlantic, with strong signal over the Norwegian Sea when northern continental areas were analyzed. Studies focused on specific regions also found similar results, for instance Gimeno et al. (2011) and Drumond et al. (2011) for the Iberian Peninsula, or studies done over European regions at higher latitudes (Nieto et al., 2007; Sodemann et al., 2008) revealed the importance of the Atlantic source. Interestingly in almost all of these studies the authors point to the effects of the atmospheric rivers as the major moisture transport mechanism from the subtropical Atlantic.

We are particularly interested in understanding which moisture source regions (depicted in Fig. 3, left panels) are reinforced during ARs associated to the five different regions. This reinforced sectors are identified in yellowish and reddish colour in maps of $(E-P)_{\mathrm{An}}$ (Fig. 3, right panels). Overall, the largest anomalies are detected in the middle of the northern Atlantic, between 20 and 40° N, with a light northward movement when the sink region is positioned at higher latitudes. The results confirm that part of the excess of moisture transported by ARs vs. the climatology comes from tropical latitudes (under the Tropic of Cancer line, 23.26° N), but the bulk additional amount

ESDD
6, 2617–2643, 2015

provided by ARs is obtained from subtropical ocean areas (i.e. between Tropic of Cancer and 35° N). The most notable anomaly in the evaporation is detected for the Iberian Peninsula, followed by the southern Scandinavia and the Netherlands region, and the lowest for the northern Scandinavia region. Each region shows differences in values of $(E-P)_{\text{An}}$ in both latitude and longitude. To understand better these patterns we quantify the anomaly values at different longitudes between 70 to 5° N and from 10 to 60° W every 10°. Figure 4 shows the different latitudinal sections for all the studied regions, values over the 90th percentile of the anomaly (Table 4) are highlighted as a bold line. We will refer to these values to compare the five areas of study. The displacement to the south of the anomaly with the longitude is a common feature for all the regions, being the longitudinal slope higher with the latitude of the sink region. So, for instance, for the northern Scandinavia (purple line) the anomalous uptake of moisture at 10° W occurs mostly between 60–48° N, while at 60° W it occurs predominantly between 40–30° N; whereas for the Iberian Peninsula (IP, red line) at 10° W the anomalous uptake occurs mainly in a band between 43–33° N and at 60° W it is particularly intense between 36–21° N. The Iberian Peninsula shows the highest values of $(E-P)_{\text{An}}$ for all the latitudes and is the region where the anomalous moisture uptake occurs further south, with local maxima partially over tropical areas. As the region is positioned more to the North the tropical source of moisture tends to be lower, but the subtropical source still dominates, particularly at central and western longitudes. A Fig. S1 in the Supplement is included to complement the information give in Fig. 4, but showing the same results for each individually domain.

It is important to put these results in light of recent works that deal with the origin of moisture in ARs. Sodemann and Stohl (2013), show that for December 2006, several ARs, reached from the subtropics to high latitudes, inducing precipitation over western Scandinavia. The sources and transport of water vapour in the North Atlantic storm track during that month were examined and revealed that the ARs were composed of a sequence of meridional excursions of water vapour. Different moisture sources where found: (1) in cyclone cores, fast turnover of water vapour by evaporation and

ESDD
6, 2617–2643, 2015

condensation were identified, leading to a rapid assimilation of water from the underlying ocean surface; (2) in the regions of long-range transport, water vapour tracers from the southern mid-latitudes and subtropics dominated over local contributions.

We acknowledge that some authors are sceptical on the far reaching origin of moisture considered ARs. Thus, Dacre et al. (2015) have looked into a selected number of cases of water vapour transport associated to North Atlantic extra-tropical cyclones in winter. The authors inferred that ARs moisture originates mostly from the water vapour in the cyclone's warm sector, not so much from long-distance transport of water vapour from the subtropics. Our long term $E-P$ analysis, confirms that, for the ARs that landfall in the western European coast, the advection of moisture linked with the ARs comes mainly from subtropical areas and, to a less extend, from mid-latitudes. In addition, a small moisture source was also found at the tropical zone.

It must be noticed that the method is not able to separate E and P entirely as it does not represent completely the evaporation (E) field, but provides only an estimation. Even so, the approach is sufficiently robust whether the method is applied at daily scale or at the monthly or ever at longer time-scales (Castillo et al., 2014), providing a useful tool to study the geographical location of moisture sources and to analyse their anomaly and possible variability.

5 Conclusions

We have undertaken a novel study regarding the moisture source of the ARs that strike different western domains in Europe in the winter half-year (ONDJFM). To achieve this goal, we have used an AR detection scheme (Lavers et al., 2012; Ramos et al., 2015) that depends entirely on the vertically integrated horizontal water vapour transport (IVT). In order to ensure a consistent detection scheme, this was applied to 3 different reference meridians (9.75° W, 4.50 and 5.25° E) into 10° sectors between 35 and 75° N. The use of 3 different meridians represents a refinement over Lavers and Villarini (2013) that only use the 10° W meridian reference. Since we are mostly interested in those ARs that make landfall in western Europe and over land, we have re-grouped the ARs previously computed (Fig. 1a and Table 1) into the following new 5 domains (Fig. 1b): (1) *Iberian Peninsula* (9.75° W; 36–43.75° N); (2) *France* (4.5° W; 43.75–50° N); (3) *UK* (4.5° W; 50–59° N); (4) *southern Scandinavia and the Netherlands* (5.25° E; 50–59° N) and (5) *northern Scandinavia* (5.25° E; 59–70° N).

The number of ARs found show a latitunal dependence with the highest values being recorded for the three merdional references 9.75° W, 4.50 and 5.25° E are 45–55, 35–45° N and 50–60° N respectively. We then considered only the ARs that make landfall in western Europe and over land into the new domains is considered, the French (140 ARs) and southern Scandinavia and the Netherlands (90 ARs) domains record the highest values while the Iberian Peninsula (21) domain record the lowest value.

The Lagrangian perspective of this work can help to give additional input regarding the effective moisture sources associated to most of the ARs that strike Europe. The moisture sources analysis ($E-P$) were evaluated taking into account the air particles residing over the western 5° from the ARs detection meridian reference mentioned above and in Table 3. The most important results obtained for the ARs moisture sources and transport can be summarized as follows:

- In general, for all the regions, the major climatological source of moisture extends along the subtropical North Atlantic, from the Florida Peninsula (northward 20° N) to each sink region. However, the mid-latitude also plays an important role as effective source of moisture with the coastal area nearest to each sink region always appearing as a local maximum of evaporation.

- The Atlantic subtropical source is reinforced during ARs where the major anomalies are detected in the middle of the northern Atlantic, between 20 and 40° N, with a slight northward movement when the sink region is positioned at higher latitudes.

ESDD
6, 2617–2643, 2015

– The most notable anomaly in the evaporation is detected for the Iberian Peninsula, following by the southern Scandinavia and the Netherlands region, and the lowest for the northern Scandinavia region.

To conclude, we show that the main sources and advection of moisture linked to ARs that strike western Europe coast have the subtropical areas as the most important ones as the moisture sources longitudes are located westward, but one must be aware also to the appearance of the tropical source, and the extra-tropical moisture sources as we move nearest the European coast. Near the sink continental areas the main source of moisture are also local as produced by the ocean vicinity.

The Supplement related to this article is available online at doi:10.5194/esdd-6-2617-2015-supplement.

Acknowledgements. Alexandre M. Ramos was supported through a postdoctoral grant (SFRH/BPD/84328/2012) from the Portuguese Science Foundation (Fundação para a Ciência e a Tecnologia, FCT). This work also was partially supported by FEDER funds through the COMPETE (Programa Operacional Factores de Competitividade) Programme and by national funds through FCT (Fundação para a Ciência e a Tecnologia, Portugal) through project STORMEx FCOMP-01-0124-FEDER-019524 (PTDC/AAC-CLI/121339/2010). Raquel Nieto acknowledges funding by the Spanish MINECO within the project TRAMO and the Galician Regional Government (Xunta) within the project THIS, both co-funding by FEDER.

References

Bao, J.-W., Michelson, S. A., Neiman, P. J., Ralph, F. M., and Wilczak, J. M.: Interpretation of enhanced integrated water vapor bands associated with extratropical cyclones: their formation and connection to tropical moisture, Mon. Weather Rev., 134, 1063–1080, 2006.
Castillo, R., Nieto, R., Drumond, A., and Gimeno, L.: Estimating the temporal domain when the discount of the net evaporation term affects the resulting net precipitation pat-

ESDD
6, 2617–2643, 2015

tern in the moisture budget using a 3-D Lagrangian approach, PLoS ONE, 9, e99046, doi:10.1371/journal.pone.0099046, 2014.
Dacre, H., Clark, P., Martinez-Alvarado, O., Stringer, M., and Lavers, D.: How do atmospheric rivers form?, B. Am. Meteorol. Soc., 96, 1243–1255, doi:10.1175/BAMS-D-14-00031.1, 2015.
Dee, D. P., Uppala, S. M., Simmons, A. J., Berrisford, P., Poli, P., Kobayashi, S., Andrae, U., Balmaseda, M. A., Balsamo, G., Bauer, P., Bechtold, P., Beljaars, A. C. M., van de Berg, L., Bidlot, J., Bormann, N., Delsol, C., Dragani, R., Fuentes, M., Geer, A. J., Haimberger, L., Healy, S. B., Hersbach, H., Hólm, E. V., Isaksen, L., Kållberg, P., Köhler, M., Matricardi, M., McNally, A. P., Monge-Sanz, B. M., Morcrette, J.-J., Park, B.-K., Peubey, C., de Rosnay, P., Tavolato, C., Thépaut, J.-N., and Vitart, F.: The ERA-Interim reanalysis: configuration and performance of the data assimilation system, Q. J. Roy. Meteorol. Soc., 137, 553–597, 2011.
Dettinger, M., Ralph, F. M., Das, T., Neiman, P. J., and Cayan, D. R.: Atmospheric rivers, floods and the water resources of California, Water, 3, 445–478, 2011.
Dettinger, M., Ralph, F. M., and Lavers, D.: Setting the stage for a global science of atmospheric rivers, Eos, 96, doi:10.1029/2015EO038675, 2015.
Drumond, A., Gimeno, L., and Nieto, R.: On the contribution of the Tropical Western Hemisphere Warm Pool source of moisture to the Northern Hemisphere precipitation through a lagrangian approach, J. Geophys. Res., 116, D00Q04, doi:10.1029/2010JD015397, 2011.
Gimeno, L., Drumond, A., Nieto, R., Trigo, R. M., and Stohl, A.: On the origin of continental precipitation, Geophys. Res. Lett., 37, L13804, doi:10.1029/2010GL043712, 2010.
Gimeno, L., Nieto, R., Trigo, R. M., Vicente, S., and Lopez-Moreno, J. I.: Where does the Iberian Peninsula moisture come from? An answer based on a Largrangian approach, J. Hydrometeorol., 11, 421–436, doi:10.1175/2009JHM1182.1, 2011.
Gimeno, L., Nieto, R., Vázquez, M., and Lavers, D. A.: Atmospheric rivers: a mini-review, Front. Earth Sci., 2, 2:2, doi:10.3389/feart.2014.00002, 2014.
Knippertz, P. and Wernli, H.: A Lagrangian climatology of tropical moisture exports to the northern hemispheric extratropics, J. Climate, 23, 987–1003, 2010.
Lavers, D. A. and Villarini, G.: The nexus between atmospheric rivers and extreme precipitation across Europe, Geophys. Res. Lett., 40, 3259–3264, 2013.
Lavers, D. A., Allan, R. P., Wood, E. F., Villarini, G., D. J., Brayshaw, and Wade, A. J.: Winter floods in Britain are connected to atmospheric rivers, Geophys. Res. Lett., 38, L23803, doi:10.1029/2011GL049783, 2011.

ESDD
6, 2617–2643, 2015

Atmospheric rivers moisture transport from a Lagrangian perspective

A. M. Ramos et al.

Lavers, D. A., Villarini, G., Allan, R. P., Wood, E. F., and Wade, A. J.: The detection of atmospheric rivers in atmospheric reanalyses and their links to British winter floods and the large-scale climatic circulation, J. Geophys. Res., 117, D20106, doi:10.1029/2012JD018027, 2012.
Liberato, M. L. R., Ramos, A. M., Trigo, R. M., Trigo, I. F., Durán-Quesada, A. M., Nieto, R., and Gimeno, L.: Moisture sources and large-scale dynamics associated with a flash flood event, in: Lagrangian Modeling of the Atmosphere, edited by: Lin, J., Brunner, D., Gerbig, C., Stohl, A., Luhar, A., and Webley, P., American Geophysical Union, Washington, D.C., doi:10.1029/2012GM001244, 2012.
Moore, B. J., Neiman, P. J., Ralph, F. M., and Barthold, F. E.: Physical processes associated with heavy flooding rainfall in Nashville, Tennessee, and vicinity during 1–2 May 2010: the role of an atmospheric river and mesoscale convective systems, Mon. Weather Rev., 140, 358–378, 2012.
Neiman, P. J., Ralph, F. M., Wick, G. A., Lundquist, J. D., and Dettinger, M. D.: Meteorological characteristics and overland precipitation impacts of atmospheric rivers affecting the west coast of North America based on eight years of SSM/I satellite observations, J. Hydrometeorol., 9, 22–47, 2008.
Nieto, R. and Gimeno, L.: Atmospheric transport towards the Iberian Peninsula in the range 3–10 days. Sources of middle-lived pollutants and aerosols, Scient. World J., 6, 1041–1047, doi:10.1100/tsw.2006.208, 2006.
Nieto, R., Gimeno, L., Gallego, D., and Trigo, R. M.: Identification of major sources of moisture and precipitation over Iceland, Meteorol. Z., 16, 37–44, 2007.
Numaguti, A.: Origin and recycling processes of precipitating water over the Eurasian continent: experiments using an atmospheric general circulation model, J. Geophys. Res., 104, 1957–1972, 1999.
Ralph, F. M. and Dettinger, M. D.: Storms, floods, and the science of atmospheric rivers, EOS T. Am. Geophys. Un., 92, 265, doi:10.1029/2011EO320001, 2011.
Ralph, F. M., Neiman, P. J., and Wick, G. A.: Satellite and CALJET aircraft observations of atmospheric rivers over the eastern North Pacific Ocean during the winter of 1997/98, Mon. Weather Rev., 132, 1721–1745, 2004.
Ralph, F. M., Coleman, T., Neiman, P. J., Zamora, R. J., and Dettinger, M. D.: Observed impacts of duration and seasonality of atmospheric-river landfalls on soil moisture and runoff in coastal northern California, J. Hydrometeorol., 14, 443–459, 2013.

ESDD
6, 2617–2643, 2015

Ramos, A. M., Trigo, R. M., Liberato, M. L. R., and Tome, R.: Daily precipitation extreme events in the Iberian Peninsula and its association with Atmospheric Rivers, J. Hydrometeorol., 16, 579–597, doi:10.1175/JHM-D-14-0103.1, 2015.

Stohl, A. and James, P. A.: Lagrangian analysis of the atmospheric branch of the global water cycle. Part I: Method description, validation, and demonstration for the August 2002 flooding in central Europe, J. Hydrometeorol., 5, 656–678, 2004.

Stohl, A., Hittenberger, M., and Wotawa, G.: Validation of the Lagrangian particle dispersion model FLEXPART against large-scale tracer experiment data, Atmos. Environ., 32, 4245–4264, 1998.

Stohl, A., Forster, C., and Sodemann, C.: Remote sources of water vapor forming precipitation on the Norwegian west coast at 60° N: a tale of hurricanes and an atmospheric river, J. Geophys. Res., 113, D05102, doi:10.1029/2007JD009006, 2008.

Sodemann, H. and Stohl, A.: Moisture origin and meridional transport in atmospheric rivers and their association with multiple cyclones, Mon. Weather Rev., 141, 2850–2868, 2013.

Sodemann, H., Schwierz, C., and Wernli, H.: Interannual variability of Greenland winter precipitation sources: lagrangian moisture diagnostic and North Atlantic Oscillation influence, J. Geophys. Res., 113, D03107, doi:10.1029/2007JD008503, 2008.

Trigo, R. M., Varino, F., Ramos, A. M., Valente, M. A., Zêzere, J. L., Vaquero, J. M., Gouveia, C. M., and Russo, A.: The record precipitation and flood event in Iberia in December 1876: description and synoptic analysis, Front. Earth Sci., 2, 2:3. doi:10.3389/feart.2014.00003, 2014

Wernli, H.: A Lagrangian-based analysis of extratropical cyclones. II: A detailed case study, Q. J. Roy. Meteorol. Soc., 123, 1677–1706, 1997.

Zhu, Y. and Newell, R. E.: A proposed algorithm for moisture fluxes from atmospheric rivers, Mon. Weather Rev., 126, 725–735, 1998.

ESDD

6, 2617–2643, 2015

Atmospheric rivers moisture transport from a Lagrangian perspective

A. M. Ramos et al.

Table 1. The vertically integrated horizontal water vapour transport (IVT) threshold and the number of persistent atmospheric rivers detected for each different domain.

	Sector	IVT threshold ($kg\,m^{-1}\,s^{-1}$)	Number of AR
Iberian Peninsula/Ireland (9.75° W)	35–45° N	621.7048	79
	45–55° N	691.5456	87
	55–65° N	614.4121	70
	65–75° N	453.4208	35
UK/France (4.50° W)	35–45° N	527.9475	113
	45–55° N	637.2342	94
	55–65° N	544.0915	98
	65–75° N	439.4734	46
Scandinavia (5.25° E)	50–60° N	524.1678	100
	60–70° N	468.0643	80

ESDD
6, 2617–2643, 2015

Table 2. The new defined atmospheric rivers landfall domains and the correspondent number of atmospheric rivers and respective number of time steps.

ARs domains	Number of ARs	Number of ARs time steps
(1) Iberian Peninsula 9.75° W; 36–43.75° N	21	117
(2) France 4.5° W; 43.75–50° N	140	665
(3) UK 4.5° W; 50–59° N	74	343
(4) Southern Scandinavia and the Netherlands 5.25° E; 50–59° N	90	423
(5) Northern Scandinavia 5.25° E; 59–70° N	83	317

ESDD
6, 2617–2643, 2015

Table 3. $E-P$ backward trajectories regions where the computation is made for all the air parcels inside it.

ARs domains	Latitude and Longitude limits
(1) Iberian Peninsula	9.75–4.75° W ; 36–43.75° N
(2) France	4.5° W–0.5° E ; 43.75–50° N
(3) UK	4.5° W–0.5° E ; 50–59° N
(4) Southern Scandinavia and the Netherlands	5.25–10.25° E ; 50–59° N
(5) Northern Scandinavia	5.25–10.25° E ; 59–70° N

ESDD
6, 2617–2643, 2015

ESDD
6, 2617–2643, 2015

Atmospheric rivers moisture transport from a Lagrangian perspective

A. M. Ramos et al.

Table 4. Percentile 90th for the anomaly values of $(E-P)>0$ field $[(E-P)_{An}]$ for each studied domain and longitude (in $mm\,day^{-1}$).

	Iberian Peninsula	France	UK	Southern Scandinavia and the Netherlands	Northern Scandinavia
10° W	0.45	0.40	0.50	0.55	0.41
20° W	0.77	0.56	0.69	0.73	0.53
30° W	0.82	0.69	0.90	0.86	0.63
40° W	0.99	0.85	0.93	0.90	0.62
50° W	0.98	0.81	0.83	0.80	0.56
60° W	1.06	0.79	0.64	0.71	0.52

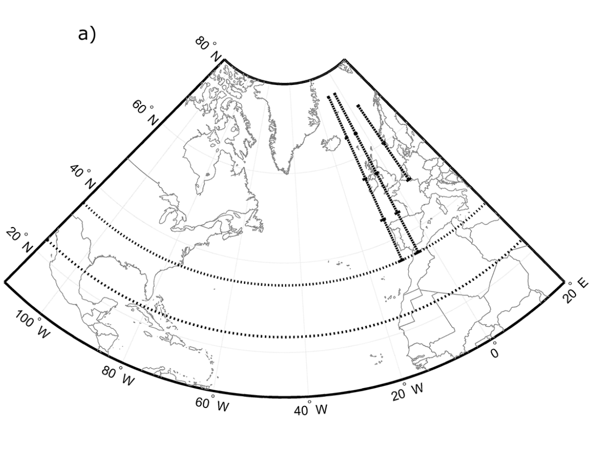

Figure 1. (a) Location of the different meridians domains and sectors in Europe used for the computation of the atmospheric rivers. **(b)** The new defined atmospheric rivers landfall domains: Iberian Peninsula (red), France (blue), UK (green), south Scandinavia (yellow) and north Scandinavia (purple). The Tropic of Cancer parallel (23.26° N) and the 35° N parallel are also shown.

ESDD
6, 2617–2643, 2015

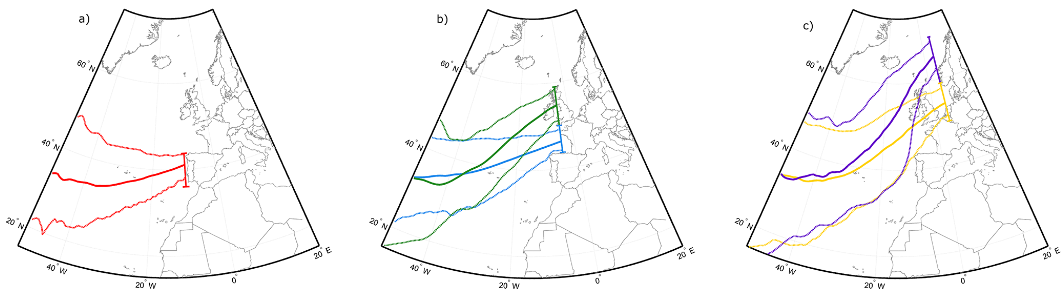

Figure 2. The median position (colour line) and the respective 90th percentile 10th percentile (dashed line) of the atmospheric rivers path along the North Atlantic Ocean before arriving to each studied domain: **(a)** Iberian Peninsula (red), **(b)** France (blue) and UK (green) and **(c)** southern Scandinavia and the Netherlands (yellow) and northern Scandinavia (purple).

ESDD

6, 2617–2643, 2015

Atmospheric rivers moisture transport from a Lagrangian perspective

A. M. Ramos et al.

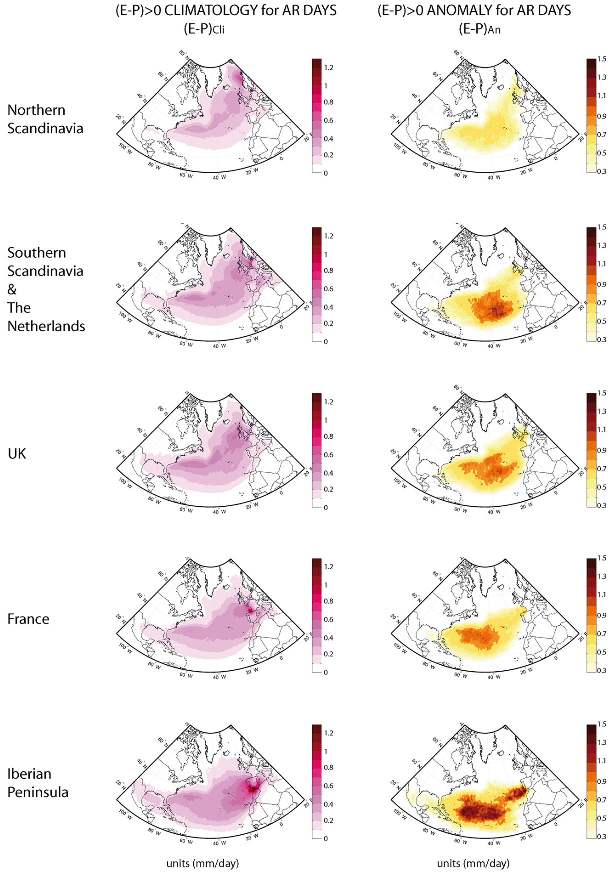

Figure 3. For each studied sink domain (Iberian Peninsula, France, UK, southern Scandinavia and the Netherlands, and northern Scandinavia) for wintertime from 1979 to 2012: Left panels: mean value of the $(E-P)>0$ field $[(E-P)_{\text{Cli}}]$, backward integrated over a 10 day period. Right panels: $(E-P)>0$ anomaly field for ARs days $[(E-P)_{\text{An}}]$. Units in mm day^{-1}.

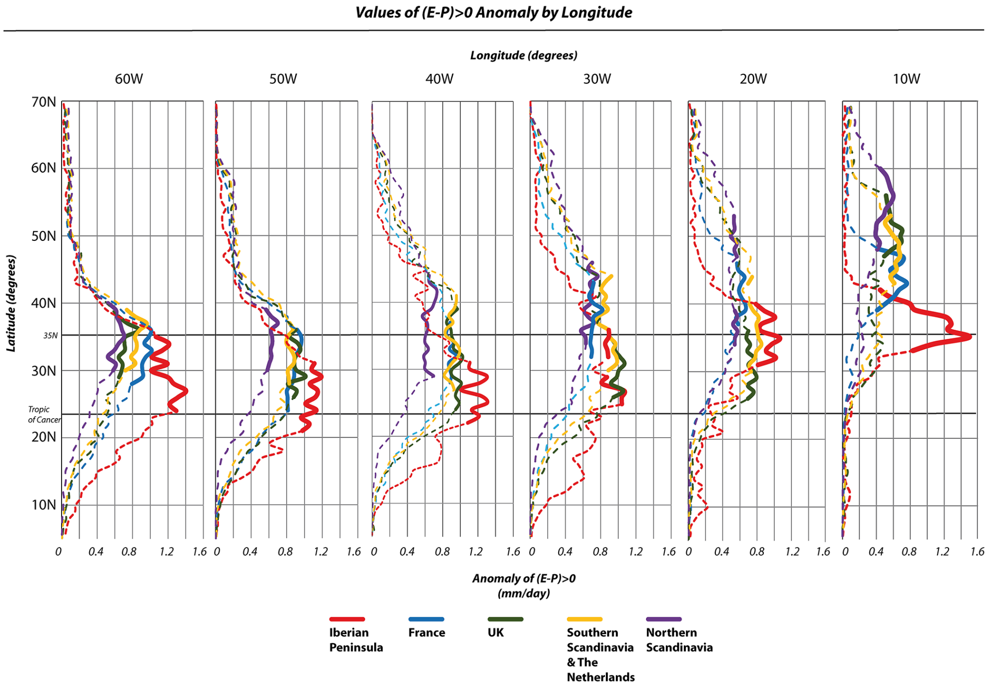

Figure 4. Longitudinal cross section of the anomaly values of $(E-P)>0$ field $[(E-P)_{\mathrm{An}}]$ for each studied domain: Iberian Peninsula (red line), France (blue), UK (green), southern Scandinavia and the Netherlands (yellow), and northern Scandinavia (purple). Bold line shows those values over the 90th percentil of each serie (values shown in Table 4). Units in $\mathrm{mm\,day^{-1}}$. The Tropic of Cancer parallel (23.26° N) and the 35° N parallel are also shown.

ESDD
6, 2617–2643, 2015